JOURNAL OF NEUROTRAUMA 27:2011–2020 (November 2010)

DOI: 10.1089/neu.2009.1226

Early and Sustained Increase in the Expression of Hippocampal IGF-1, But Not EPO, in a Developmental Rodent Model of Traumatic Brain Injury

Michelle E. Schober,[1] Benjamin Block,[2] Joanna C. Beachy,[2] Kimberly D. Statler,[1,3] Christopher C. Giza,[4] and Robert H. Lane[2]

Abstract

Pediatric traumatic brain injury (pTBI) is the leading cause of traumatic death and disability in children in the United States. Impaired learning and memory in these young survivors imposes a heavy toll on society. In adult TBI (aTBI) models, cognitive outcome improved after administration of erythropoietin (EPO) or insulin-like growth factor-1 (IGF-1). Little is known about the production of these agents in the hippocampus, a brain region critical for learning and memory, after pTBI. Our objective was to describe hippocampal expression of EPO and IGF-1, together with their receptors (EPOR and IGF-1R, respectively), over time after pTBI in 17-day-old rats. We used the controlled cortical impact (CCI) model and measured hippocampal mRNA levels of EPO, IGF-1, EPOR, IGF-1R, and markers of caspase-dependent apoptosis (bcl2, bax, and p53) at post-injury days (PID) 1, 2, 3, 7, and 14. CCI rats performed poorly on Morris water maze testing of spatial working memory, a hippocampally-based cognitive function. Apoptotic markers were present early and persisted for the duration of the study. EPO in our pTBI model increased much later (PID7) than in aTBI models (12 h), while EPOR and IGF-1 increased at PID1 and PID2, respectively, similar to data from aTBI models. Our data indicate that EPO expression showed a delayed upregulation post-pTBI, while EPOR increased early. We speculate that administration of EPO in the first 1–2 days after pTBI would increase hippocampal neuronal survival and function.

Key words: apoptosis; controlled cortical impact; erythropoietin receptor; insulin-like growth factor-1 receptor; neurocognitive impairment

Introduction

In the United States, pediatric traumatic brain injury (pTBI) is the leading cause of traumatic death and disability in children 1–14 years of age (Langlois et al., 2006), affecting nearly half a million children each year (Langlois et al., 2005). Survivors often have neurocognitive sequelae (Yeates et al., 2002, 2005), such as impairments in learning and memory. Despite the magnitude of the problem, no clinical therapies in use today directly improve the learning and memory impairments resulting from pTBI.

Normal learning and memory requires intact function of the hippocampus, a part of the brain that is particularly vulnerable to TBI (Gao et al., 2008). After TBI, hippocampal neuronal death is frequently associated with impaired neurological function in adults (Rao et al., 2001) and immature rats (Huh et al., 2008; Tsuru-Aoyagi et al., 2009). Even though a direct relationship between neuronal survival and cognition is lacking (Royo et al., 2007), therapies that improve neuronal survival often also improve cognitive function after trauma in adults (Hoane et al., 2009; Rao et al., 2001) and immature rats (Sonmez et al., 2007; Tsuru-Aoyagi et al., 2009).

An important mechanism of neuronal death after TBI is apoptosis (Rink et al., 1995; Zhang et al., 2005). Experimental studies suggest that apoptosis is the major contributor to a poor neuropathological outcome after trauma in the immature brain (Bittigau et al., 2004). In pTBI models, apoptotic cell death peaked in the first 24–48 hours (Bayly et al., 2006; Bittigau et al., 1999), and subsided after the first 5 days (Bittigau et al., 1999), suggesting that the impact of any anti-apoptotic

[1]Department of Pediatrics, Division of Critical Care, and [2]Division of Neonatology, University of Utah School of Medicine, [3]The Brain Institute, University of Utah, Salt Lake City, Utah.
[4]University of California–Los Angeles (UCLA) Brain Injury Research Center, Division of Pediatric Neurology and Department of Neurosurgery, David Geffen School of Medicine at UCLA, Los Angeles, California.

intervention would be greatest if present during this window of opportunity.

Erythropoietin (EPO) and insulin-like growth factor-1 (IGF-1) are anti-apoptotic agents with known neuroprotective properties (Dame et al., 2001; Russo et al., 2005). EPO and IGF-1, as well as their respective receptors (EPOR and IGF-1R), are produced in the hippocampus of both adult and immature animals (Russo et al., 2005).

EPO, EPOR (Liao et al., 2008), and IGF-1 (Li et al., 1998; Walter et al., 1997) are upregulated by TBI in adult rodents, while effects on IGF-1R are variable (Madathil et al., 2010; Sandberg Nordqvist et al., 1996; Walter et al., 1997). To our knowledge, no published studies have addressed the endogenous expression of EPO, EPOR, or IGF-1R mRNA after TBI in immature animals. A better understanding of this response would facilitate future interventional studies using EPO and/or IGF-1 after experimental pTBI. Indeed, in adult animals, administration of either EPO (Lu et al., 2005) or IGF-1 (Saatman et al., 1997) is associated with improved functional and histological outcome after TBI.

Our objective was to describe endogenous hippocampal expression of EPO, EPOR, IGF-1, and IGF-1R over time after injury in a pTBI model. Based on adult data, we hypothesized that in the hippocampus, both EPO and EPOR expression would increase, peaking at 24 h after injury, and that IGF-1 would peak at post-injury day 3 (PID 3), while IGF-1R would not change.

To test our hypotheses, we used an established model of TBI that involves the delivery of a controlled cortical impact (CCI). The rat CCI model, as first described by Dixon and associates (Dixon et al., 1991), is a well-characterized and accepted experimental paradigm that produces hippocampal neuronal death and impaired learning and memory. We adopted injury parameters similar to those used by Adelson and colleagues, who modified the CCI paradigm for use in 17-day-old rats (Adelson et al., 1998). Similarly to findings in adult rats, hippocampal neuronal death has been found after CCI in 17-day-old rats (Robertson et al., 2007). Given that relatively few studies (Hickey et al., 2007; Ochalski et al., 2010) report functional outcomes after CCI induced using comparable parameters, we used Morris water maze (MWM) testing to determine if impaired cognitive outcome occurred after CCI in our study.

Using dissected hippocampi, we measured mRNA levels of EPO, EPOR, IGF-1, and IGF-1R on PID 1, 2, 3, 7, and 14. EPO and IGF-1 protein levels were obtained at selected time points. Finally, given that age and type of injury may modulate the effect of TBI on markers of apoptosis, we measured bax, bcl2, and p53 mRNA in CCI hippocampi at the same time points at which we measured EPO and IGF-1 mRNA.

Methods

Animals

All experimental protocols were approved by the Animal Care and Use Committee at the University of Utah, in accordance with U.S. National Institutes of Health guidelines and carried out at the University of Utah. All surgical procedures were performed using aseptic technique.

Briefly, male Sprague-Dawley rats were obtained from Charles River Laboratories (Raleigh, NC) on post-natal day (PND) 7–10. We chose to study only males to eliminate any potential confounding effects of gender. The rats were housed in litters of 10 with the lactating dam until weaning on PND 21–23. After weaning, the rats were housed 3–5 per cage and allowed free access to food and water. All cages were kept in a temperature- and light-controlled (12 h on/12 h off) environment.

The three experimental groups were CCI, sham, and naive. We included naïve animals to control for expected changes in EPO/EPOR (Dame et al., 2001; Sola et al., 2005), and IGF-1/IGF-1R (Breese et al., 1994) expression over time in the developing animal. In order to control for maternal rearing characteristics, randomization was distributed evenly within litters. The rats were randomized to experimental group on the day of surgery, at age PND 17, at which time the rats underwent CCI, sham craniotomy, or were left with the dam (naïve). We chose PND 17 because the maturation state of the rodent brain at this age is comparable to the human infant and young toddler (Dobbing and Sands, 1979; Rice and Barone, 2000), the population most commonly at risk for cognitive deficits after TBI (Anderson et al., 2005; Bittigau et al., 2004).

Hippocampi were collected at PID 1, 2, 3, 7, and 14 for molecular studies. MWM testing was performed on PID 14–18.

Controlled cortical impact procedure

At least two litters of 10 rats each were used to generate the numbers needed per group (6 rats per group for molecular studies and 8 rats per group for functional testing) for each time point in our study. On PND 17, rats undergoing CCI ($n = 3$–4/litter) were anesthetized with 3% isoflurane for induction, followed by 2–2.5% isoflurane for the duration of surgical preparation, using a VetEquip Bench Top Isoflurane Anesthesia System (Pleasanton, CA). Core temperature was monitored via a rectal probe and continuously controlled at $37 \pm 0.5^{\circ}$C using a servo-controlled heating pad. Oxygenation, heart rate, and respiratory rate were monitored using femoral probe pulse oximetry (Mousox®; Starr Life Sciences, Oakmont, PA).

The rat was placed into a stereotaxic frame (David Kopf, Tujunga, CA). After shaving, prepping with povidone iodine, and incising the scalp, a craniotomy (6×6-mm) was performed over the left parietal cortex (centered around a point 4 mm posterior and 4 mm lateral to the bregma) using a high-speed dental drill. Care was taken not to perforate the dura. Once the craniotomy was complete, anesthesia was reduced to 1% isoflurane for a 5-min equilibration period. CCI was then delivered (Pittsburgh Precision Instruments, Pittsburgh, PA) to the left parietal cortex using a 5-mm rounded tip to deliver a 2-mm deformation at 4 m/sec velocity and 100 msec duration. Immediately after CCI, isoflurane was increased to 2–2.5%, and the bone flap was replaced and secured with dental cement (Patterson Dental, Salt Lake City, UT). The scalp incision was sutured, and triple antibiotic ointment and bupivacaine 0.25% were applied topically. Isoflurane was stopped, and the rats were allowed to recover in a temperature-controlled chamber. Once fully awake, the rats were returned to their dams and littermates. Sham rats ($n = 3$–4/litter) underwent identical surgical craniotomy, equilibration, and closure procedures without CCI. Naïve rats (3/litter) underwent randomization with no further intervention. Blood gas determination was made using the I-Stat® system (Abbott Laboratories, Abbott Park, IL) via left ventricular puncture from a separate cohort of

anesthetized CCI ($n = 4$) and sham ($n = 4$) rats after experimental interventions were completed.

Tissues

The rats were anesthetized with intraperitoneal (IP) xylazine (8 mg/kg) and ketamine (40 mg/kg), and killed by swift decapitation ($n = 6$ per group). After brain removal, the hippocampus was quickly dissected out on ice. The left (or ipsilateral to injury) hippocampus from CCI and sham animals was labeled either CCIipsi or Shamipsi, respectively. The right (or contralateral to injury) hippocampus from CCI and sham animals was labeled CCIcon or Shamcon, respectively. Given that CCI produces diffuse injury to the immature brain (Gobbel et al., 2007), we chose to study the two hippocampi separately, as their response to trauma could be different. The two hippocampi from each naïve animal were not analyzed separately, as genomic microarray studies have not disclosed differences between left and right hippocampi (Stansberg et al., 2007). Tissues were snap frozen in liquid nitrogen and stored at −80°C. Ground frozen tissue was used to make cDNA or protein, as detailed below.

RNA isolation and real-time RT-PCR

Hippocampal mRNA levels of EPO, EPOR, IGF-1, IGF-1R, p53, bax, and bcl2 were measured by real-time RT-PCR. In brief, total RNA was extracted with Nucleospin II (Macherey-Nagel Inc., Bethlehem, PA), treated with DNase I (Ambion, Austin, TX), and quantified by spectrophotometry (NanoDrop ND-1000; NanoDrop Technologies, Wilmington, DE). Sample integrity was confirmed by gel electrophoresis. cDNA was synthesized from 1 μg of DNase-treated total RNA. cDNA- and gene-specific probes and primers were added to TaqMan universal PCR master mix (Applied Biosystems, Carlsbad, CA), and samples were run on the 7900HT Sequence Detection System (Applied Biosystems).

Real-time RT-PCR quantification was then performed with TaqMan GAPDH as an internal control. The primers and probes used were from Applied Biosystems, as follows: for EPO, Rn01481376_m1, and for EPOR, Rn00566533_m1; for IGF-1, Rn00710306_m1, and for IGF-1R, Rn01477918_m1.

Primer pairs were designed for the remaining genes, as follows: bcl-2 forward primer, 5′-CAG GAT AAC GGA GGC TGG G-3′; reverse primer, 5′-GAA ATC AAA CAG AGG TCG CAT G-3′; probe, 5′-TGC CTT TGT GGA ACT ATA TGG CCC CA-3′; bax forward primer, 5′-TGG TTG CCC TCT TCT ACT TTG C-3′; reverse primer, 5′-TGA TCA GCT CGG GCA CTT TA-3′; probe, 5′-AAC TGG TGC TCA AGG CCC TGT GCA-3′; p53 forward primer, 5′-CCA CCC GGA TAA GAT GTT GG-3′; reverse primer, 5′-AGG AGC GAC GAC CAG GCC GTC ACC ATC A-3′; probe, 5′-AGT CAG TGG TGC CGG AGA TG-3′.

For each set of reactions, samples were run in quadruplicate. Relative quantification of PCR products was based on value differences between the target and GAPDH control by the comparative threshold cycle method (TaqMan Gold RT-PCR manual; Applied Biosystems).

Protein isolation and determination of EPO and IGF-1 proteins

For EPO protein determination, total protein samples were used. Total protein samples were extracted by homogenizing hippocampi in ice-cold lysis buffer (150 mM NaCl, 50 mM Tris [pH 7.4], 1 mM EDTA, 0.5% Na-deoxycholate, and 1% Igepal CA-630) with protease inhibitors (Roche Applied Science, Indianapolis, IN). After centrifugation at 13,000 rpm at 4°C for 10 min, the supernatants were stored at −80°C until use. Protein concentration was determined by a colorimetric assay, the bicinchoninic acid (BCA) method (Pierce Protein Research Products, Rockford, IL), and used to calculate volume for equal protein loading. Proteins were separated by SDS PAGE using Criterion XT Precast 4–12% Bis-Tris Gels (Bio-Rad, Hercules, CA), followed by transfer to PVDF membranes in CAPS buffer (10 mM 3-cyclohexylamino-1-propane sulfonic acid, 20 v/v% methanol, pH 11), at room temperature. After the membranes were blocked with 5% milk in Tris-buffered saline and 0.1% Tween 20 (TBST) at room temperature for 1 h, bound proteins were exposed to specific antibodies against EPO (rabbit polyclonal 1:200, sc-7956; Santa Cruz Biotechnology, Santa Cruz, CA) for 1 h at room temperature. After extensive washing in TBST, a 1:5000 dilution of goat anti-rabbit HRP secondary antibody (Cell Signaling Technology, Beverly, MA) was applied, and incubated for 1 h at room temperature. After extensive washing, signals were detected with Western Lightning ECL (PerkinElmer Life Sciences, Waltham, MA), and quantified relative to GAPDH (rabbit monoclonal 1:5000, 14C10; Cell Signaling Technology) by densitometry on a Kodak Image Station 2000R (Eastman Kodak/SIS, Rochester, NY).

For IGF-1 protein determination by ELISA, IGF-1 was freed from its binding proteins by homogenizing frozen hippocampal tissue in cold 1 N acetic acid, and the samples were subjected to boiling, freezing, and lyophilization. After reconstituting with PBST, the samples were placed in an ultrasound bath and vortexed thoroughly. After settling, the supernatant was aliquoted and stored at −80°C until use. Protein concentration was again determined by the BCA method (Pierce Protein Research Products) and used to normalize ELISA IGF-1 results.

The Quantikine® Rat/Mouse IGF-1 Immunoassay kit (R&D Systems Inc., Minneapolis, MN) was used to assay IGF-1 levels in the samples. ELISAs were performed according to the manufacturer's instructions. Briefly, microplates were precoated with the first primary monocolonal antibody. Assay diluents were added to each well of the microplate (50 μL/well). Standard control samples were diluted serially (1:2) from 6–0 ng/mL, or with the respective calibrator diluents, and plated to two columns of wells (50 μL/well) designated for standard curve in every plate. The frozen samples for ELISA were thawed on ice, and every sample was plated in duplicate for measurement of each of the factors. Following a 2-h incubation at room temperature, the wells were rinsed in wash buffer and treated with an enzyme-linked second primary antibody solution for 2 h. The second primary antibody was a polyclonal IGF-1 antibody conjugated to HRP in the IGF-1 detection kit. The wells were rinsed in wash buffer and a substrate solution was added to the wells and incubated in the dark for 30 min. The color reaction was stopped with 1 M hydrochloric acid. The optical density of each well was measured using the GENiosPro microplate reader (Tecan, Research Triangle Park, NC). The intensity of color was measured at a wavelength of 450 nm. In order to correct for optical imperfections in the plate, readings at 540 nm were subtracted from readings at 450 nm. The standard curve was

used to assess the validity of the protocol and to determine the relative concentrations of IGF-1. Values in all samples were normalized per milligram of protein assayed.

Morris water maze testing

The pool containing the submerged platform was located in a dimly lit room and surrounded by visual cues. The submerged platform was positioned in one of the four equal pool quadrants. The starting quadrant was varied over the four daily trials per day, using the same pattern on a given day for all study groups ($n = 6$–8/group). Serial testing (four trials per day, maximum swim time 120 sec per trial, 4-min rest between trials) was performed for 5 days with a submerged platform, from PID 14 to PID 18. Each trial was recorded using automated video tracking and data analysis equipment from the HVS Tracking System. Latency to find the platform, swim speed, swim path, and thigmotaxis (time spent swimming close to the sides of the pool) were recorded for each trial. The water temperature was maintained at $26 \pm 2^{\circ}$C.

Statistical analysis

All data are expressed as mean $\pm$ SE and/or as percentage of control. Data were analyzed using analysis of variance (ANOVA), with $p < 0.05$ defined as the cutoff for statistical significance, using Statview software. MWM data were analyzed using repeated measures ANOVA to account for multiple measurements over time. To adjust for multiple comparisons between the three groups, Tukey's Honestly Significant Difference (HSD) method was used.

Results

Overall survival for the study was 93.3% for CCI rats, 94% for sham rats, and 100% for naïve rats. All deaths occurred during anesthesia. Rectal temperatures ($37.4 \pm 0.5^{\circ}$C for TBI rats and $37.6 \pm 0.6^{\circ}$C for sham rats) did not differ between groups. Both CCI and sham animals maintained similar heart rates (300–360 and 310–350 bpm), respiratory rates (33–52 and 34–48 bpm), and oxygen saturation levels (95–99% and 96–98%), respectively, during the surgical procedures. Similarly, blood gas values obtained at the end of surgery or sham surgery were no different between CCI and sham animals (pH 7.34 ± 0.01 and 7.33 ± 0.02). All groups demonstrated equal and adequate daily weight gain during the experimental period at all time points, with the exception of PID 3, and there was no significant difference between weights. At PID 3 the weight of CCI rats was less than that of naïve rats ($p = 0.03$), but no different from that of sham rats.

mRNA results

Statistical significance was calculated using all five groups, as outlined above. We found no differences in gene expression between naïve, Shamipsi, or Shamcon hippocampi. Results for CCIcon and CCIipsi are thus presented as percentages of the levels in sham animals. CCIcon results were usually no different from sham animals. Thus any significant differences between CCIcon and sham animals are reported exclusively in the text. Graphical results portray only CCIipsi (relative to sham and/or CCIcon) values. GAPDH mRNA expression did not vary between groups at any time point.

IGF-1 mRNA (Fig. 1) increased in CCIipsi relative to sham as early as PID 1 ($132 \pm 8\%$ of sham; $p < 0.0001$). IGF-1 peaked at PID 3 ($350 \pm 68\%$ of sham; $p < 0.0001$). Hippocampal expression of IGF-1 mRNA remained increased in CCIipsi at least up to PID 14 ($165 \pm 20\%$ of sham; $p < 0.05$). IGF-1 mRNA increased relative to CCIcon at PID 1 (132 ± 8 versus $102 \pm 6\%$ of sham), PID 2 (229 ± 13 versus $79 \pm 4\%$ of sham), PID 3 (350 ± 68 versus $145 \pm 6\%$ of sham), and PID 7 (206 ± 15 versus $98 \pm 8\%$ of sham; $p \leq 0.001$ for all four time points).

CCI decreased IGF-1R in CCIipsi at PID 1 and PID 2 (65 ± 4 and $65 \pm 7\%$ of sham; $p < 0.01$ for both), followed by an increase at PID 3 ($146 \pm 10\%$ of sham; $p < 0.0001$), after which expression was unchanged relative to sham animals (Fig. 2). As shown, CCI affected IGF-1R mRNA levels similarly in both hippocampi except at PID 1 and 7. CCIipsi mRNA decreased relative to CCIcon (65 ± 4 versus $73 \pm 2\%$ of sham; $p < 0.01$) at

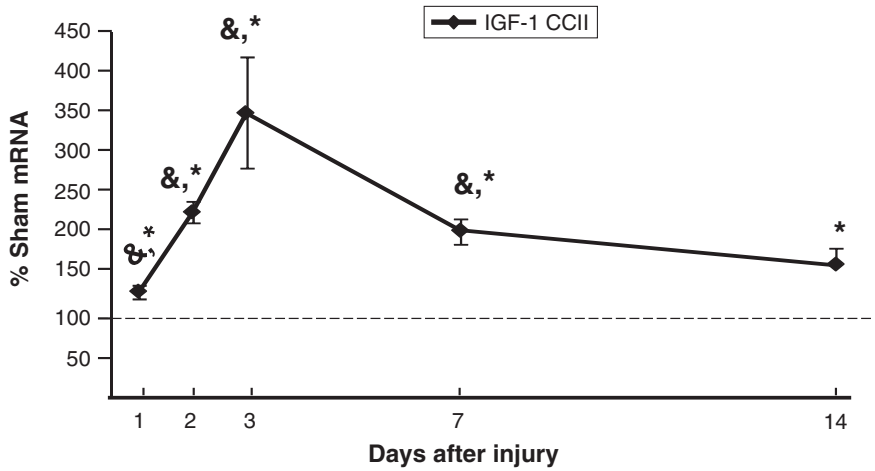

FIG. 1. Graph depicting IGF-1 mRNA in the CCI hippocampus ipsilateral to injury (CCII) obtained at post-injury days (PID) 1, 2, 3, 7, and 14, presented as a percentage of corresponding sham mRNA levels. The dashed line represents 100% of sham IGF-1 mRNA. CCII IGF-1 mRNA increased relative to both sham and CCIcon at PID 1, 2, 3, and 7, and relative to sham at PID 14. Results are presented as percentages of sham mRNA $\pm$ standard error of the mean; $n = 6$; $^*p < 0.05$ relative to sham animals; $\&p < 0.05$ relative to CCI con animals; IGF-1, insulin-like growth factor-1; CCI, controlled cortical impact).

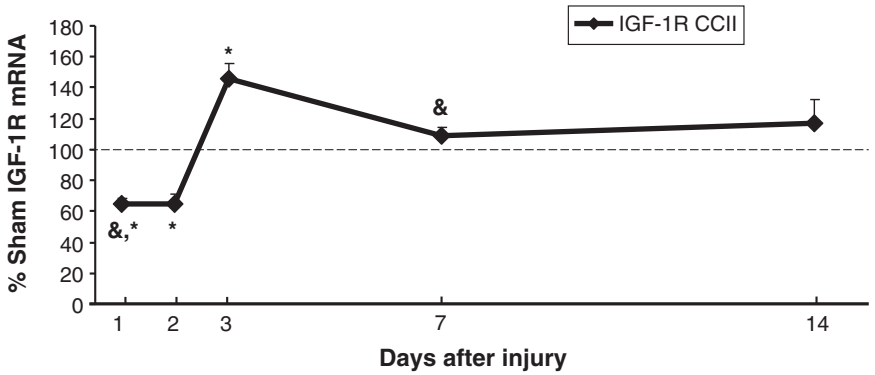

FIG. 2. Graph depicting IGF-1 receptor (IGF-1R) mRNA in CCI hippocampus ipsilateral to injury (CCII) obtained at post-injury days (PID) 1, 2, 3, 7, and 14, presented as a percentage of corresponding sham mRNA level. The dashed line represents 100% of sham IGF-1R mRNA. IGF-1R decreased in CCII relative to sham animals at PID 1 and 2, and then increased at PID 3, after which expression was unchanged. CCII IGF-1R decreased and increased, relative to CCIcon, at PID 1 and 7, respectively. Results are presented as percentages of sham mRNA ± standard error of the mean; $n = 6$; *$p < 0.05$ relative to sham animals; &$p < 0.05$ relative to CCIcon; IGF-1, insulin-like growth factor-1; CCI, controlled cortical impact).

PID 1, while CCIipsi mRNA increased relative to CCIcon (109 ± 5 versus 91 ± 5% of sham; $p < 0.01$) at PID 7. We did find differences between CCIcon and sham for this gene. Namely, CCIcon IGF-1R mRNA decreased at PID 1 and PID 2 (to 73 ± 2 and 56 ± 4% of sham; $p < 0.001$), and increased at PID 3 (141 ± 7 of sham; $p < 0.0001$).

EPO mRNA in CCIipsi showed a strong trend towards an increase at PID 3 (147 ± 12% of sham; $p = 0.05$), was increased at PID 7 (179 ± 32% of sham; $p < 0.05$), and was no different from sham at PID 14. CCIipsi EPO mRNA increased relative to CCIcon at PID 3 (147 ± 12 versus 99 ± 9% sham; $p < 0.05$), and PID 7 (179 ± 32 versus 109 ± 13%; $p < 0.05$), as shown in Figure 3.

Interestingly, EPOR mRNA in CCIipsi increased as early as PID 1 (241 ± 14% of sham animals; $p < 0.0001$), and PID 2 (309 ± 41% of sham; $p < 0.0001$), peaked at PID 3 (626 ± 99% of sham; $p < 0.0001$), and remained elevated at PID 7 (479 ± 105% of sham; $p < 0.0001$), and PID 14 (280 ± 55% of sham; $p < 0.01$), as shown in Figure 4. CCIipsi EPOR mRNA was also increased relative to CCIcon at all five time points. CCIcon EPOR mRNA levels were only different from sham animals at one time point, at PID 1 (138 ± 6% of sham; $p < 0.01$).

p53 mRNA levels in CCIipsi were increased at PID 3 (144 ± 8%; $p < 0.0001$), PID 7 (135 ± 9%; $p < 0.001$), and PID 14 (137 ± 9%; $p < 0.01$) relative to sham animals. At PID 3 and 7, CCIipsi p53 mRNA was also increased relative to CCIcon ($p < 0.01$ and $p = 0.0001$, respectively), as shown in Figure 5. bax mRNA expression was increased at PID 2 (133 ± 5% of sham; $p < 0.05$), and at PID 14 (121 ± 9% of sham; $p < 0.05$;

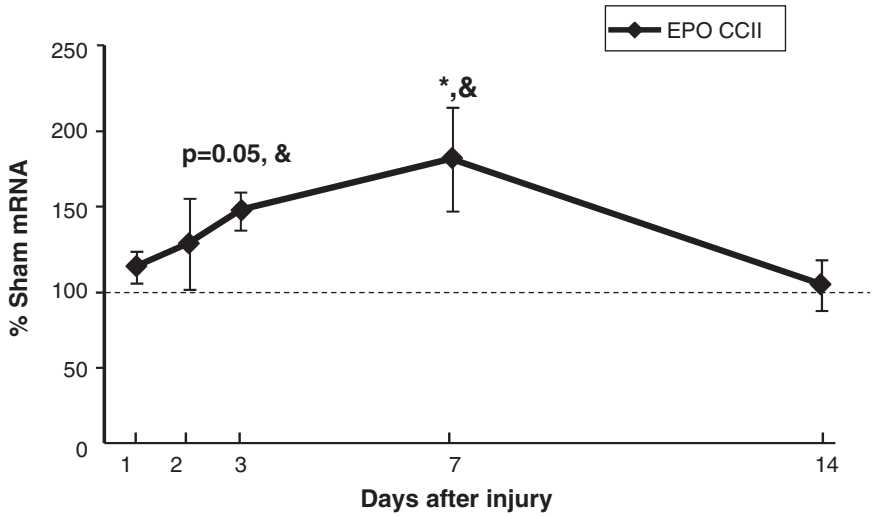

FIG. 3. Graph depicting EPO mRNA in CCI hippocampus ipsilateral to injury (CCII) obtained at post-injury days (PID) 1, 2, 3, 7, and 14, presented as a percentage of corresponding sham mRNA levels. The dashed line represents 100% of sham EPO mRNA. CCII EPO trended towards an increase at PID 3 ($p = 0.05$), and was increased at PID 7, relative to sham animals. CCII EPO increased relative to CCIcon at PID 3 and 7. Results are presented as percentages of sham mRNA ± standard error of the mean; $n = 6$; *$p < 0.05$ relative to sham animals; &$p < 0.05$ relative to CCIcon; EPO, erythropoietin; CCI, controlled cortical impact).

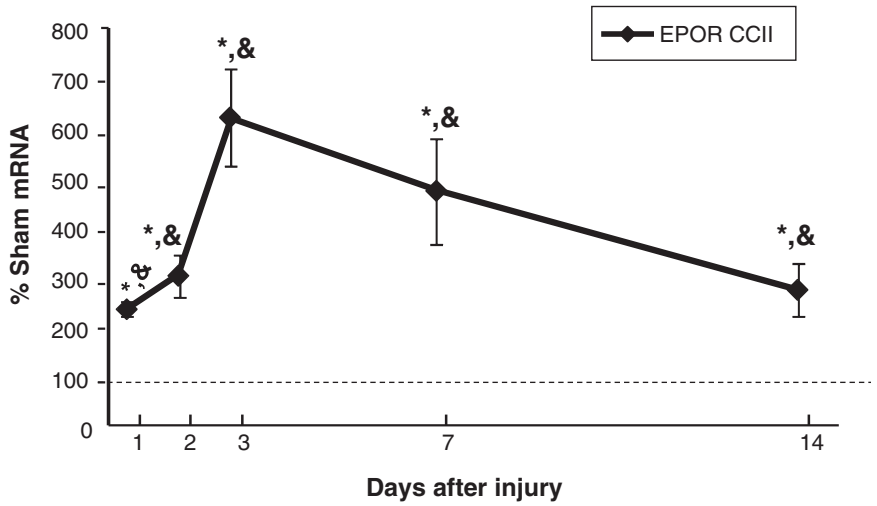

FIG. 4. Graph depicting EPOR mRNA in CCI hippocampus ipsilateral to injury (CCII) obtained at post-injury days (PID) 1, 2, 3, 7, and 14, presented as a percentage of corresponding sham mRNA levels. The dashed line represents 100% of sham EPOR mRNA. EPOR was increased relative to sham and to CCIcon as early as PID 1, peaked at PID 3, and remained elevated at least until PID 14. Results are presented as percentage of sham mRNA ± standard error of the mean; $n = 6$; **$p < 0.05$ relative to Sham; &$p < 0.05$ relative to CCIcon; EPOR, erythropoietin receptor; CCI, controlled cortical impact).

Fig. 6). CCIcon bax mRNA briefly increased relative to sham at PID 3 (119 ± 6% of sham; $p < 0.01$), and then decreased at PID 7 (79 ± 3% of sham; $p < 0.01$). For bcl2, CCIipsi mRNA expression decreased at PID 1 relative to sham (92 ± 3% of sham; $p = 0.01$), and relative to CCI con (92 ± 3 versus 99 ± 2% of sham; $p < 0.05$), as shown in Figure 7. In a given tissue, the ratio of pro-apoptotic bax to anti-apoptotic bcl2 is important in determining the direction of apoptotic forces (Agarwal et al., 2004). In our study, the increased bax:bcl2 ratio seen during the first 2 days after injury supports increased apoptosis during this period.

Protein results

Consistent with mRNA results, CCIipsi EPO protein was no different from sham at PID 2, but was greater than sham at PID 7 (0.39 ± 0.01 versus 0.18 ± 0.03; $p = 0.0003$), as shown in Figure 8. GAPDH protein levels did not differ between groups.

We measured average values of IGF-1 protein (picograms IGF-1/mg total protein per sample) per group ($n = 6$) at three time points. We found no differences between CCIipsi and sham animals at PID 2 (1118 ± 470 versus 427 ± 66 pg/mg), PID 7 (821 ± 125 versus 693 ± 203 pg/mg), or PID 14 (1271 ± 122 versus 1000 ± 286 pg/mg).

Morris water maze results

MWM testing demonstrated increased average latency in CCI animals on testing days 3 (relative to sham) and 4 (relative to naïve), as shown in Figure 9. Swim speed was no different between groups (0.171 ± 0.015, 0.165 ± 0.003, and

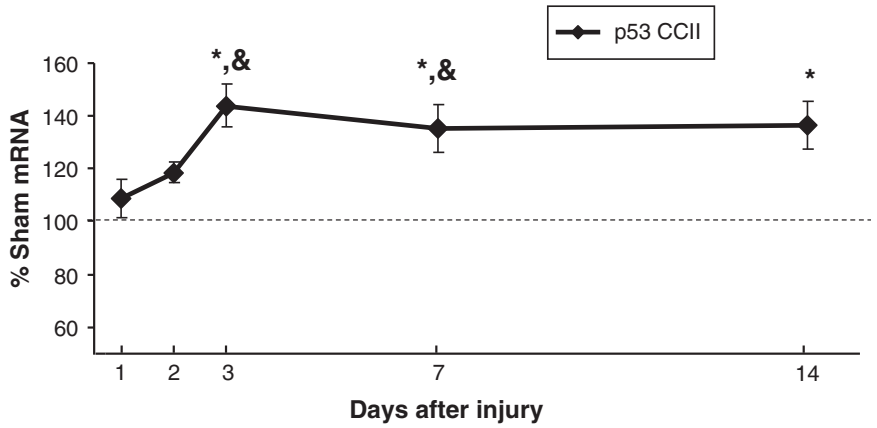

FIG. 5. Graph depicting p53 mRNA in CCI hippocampus ipsilateral to injury (CCII) obtained at post-injury days (PID) 1, 2, 3, 7, and 14, presented as a percentage of the corresponding sham mRNA level. The dashed line represents 100% of sham p53 mRNA. CCII p53 mRNA increased at PID 3 and PID 7 relative to both sham and CCIcon, and at PID 14 relative to sham animals. Results are presented as percentage of sham mRNA ± standard error of the mean; $n = 6$; *$p < 0.05$ relative to sham; &$p < 0.05$ relative to CCIcon; CCI, controlled cortical impact).

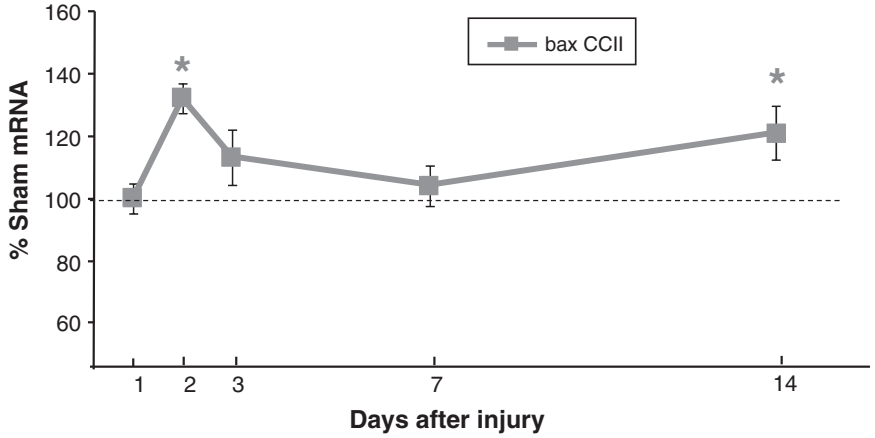

FIG. 6. Graph depicting bax mRNA in CCI hippocampus ipsilateral to injury (CCII) obtained at post-injury days (PID) 1, 2, 3, 7, and 14, presented as a percentage of corresponding sham mRNA levels. The dashed line represents 100% of sham bax mRNA. CCII bax mRNA was increased at PID 2 and at PID 14. Results are presented as percentage of sham mRNA ± standard error of the mean; $n = 6$; *$p < 0.05$ relative to sham animals; CCI, controlled cortical impact).

0.172 ± 0.006 m/sec for CCI, naïve, and sham animals, respectively). Similarly we found no differences in swim path or thigmotaxis.

Discussion

We found that IGF-1 mRNA, as predicted, peaked at PID 3. In accordance with our hypothesis, EPOR increased at PID 1, but it peaked later than expected (PID 3). Contrary to our predictions, we found that EPO expression did not increase in the first 24 h, but rather did so at PID 7. In accordance with EPO mRNA results, EPO protein was unchanged at PID 2, and was increased at PID 7.

Interestingly, gene expression in the hippocampus contralateral to injury was generally no different from sham animals. In particular, our findings suggest that little to no compensatory increased EPO and IGF-1 production occurs in the contralateral hippocampus during the first 2 weeks after CCI. This was not entirely unexpected, because although CCI in immature rats produces diffuse damage to the entire brain, it is more severe on the side of impact (Gobbel et al., 2007), with more marked neuronal loss in the hippocampal subfields ipsilateral to the impact (Robertson et al., 2007).

Expression of all our genes of interest was no different between shams and naïves. This suggests that CCI alone, and not the associated experimental paradigm, altered the expression of our genes of interest. This finding is particularly important for IGF-1 and EPO, which are subject to developmental changes. Hippocampal EPO expression in the rat, and IGF-1 expression in the mouse, were both highest at birth and then decreased (Sanchez et al., 2009; Zhang et al., 2007).

Our results compare favorably with the sparse data available on IGF-1 expression after experimental TBI in immature animals; similarly to our findings, IGF-1 mRNA increased at PID 3 and PID 7 in a model of penetrating brain injury using D14 mice (Li et al., 1998).

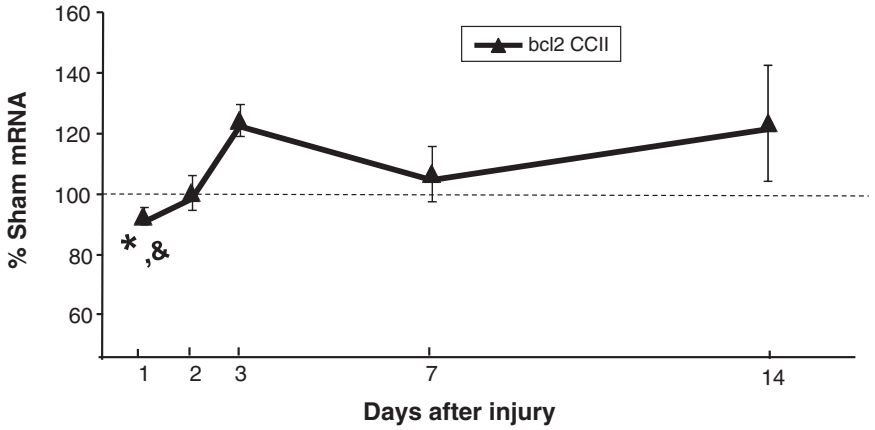

FIG. 7. Graph depicting bcl2 mRNA in CCI hippocampus ipsilateral to injury (CCII) obtained at post-injury days (PID) 1, 2, 3, 7, and 14, presented as a percentage of corresponding sham mRNA levels. The dashed line represents 100% of sham bcl2 mRNA. CCII bcl2 mRNA was decreased relative to sham and to CCIcon at PID 1. Results are presented as percentages of sham mRNA ± standard error of the mean; $n = 6$; *$p < 0.05$ relative to sham; &$p < 0.05$ relative to CCIcon; CCI, controlled cortical impact).

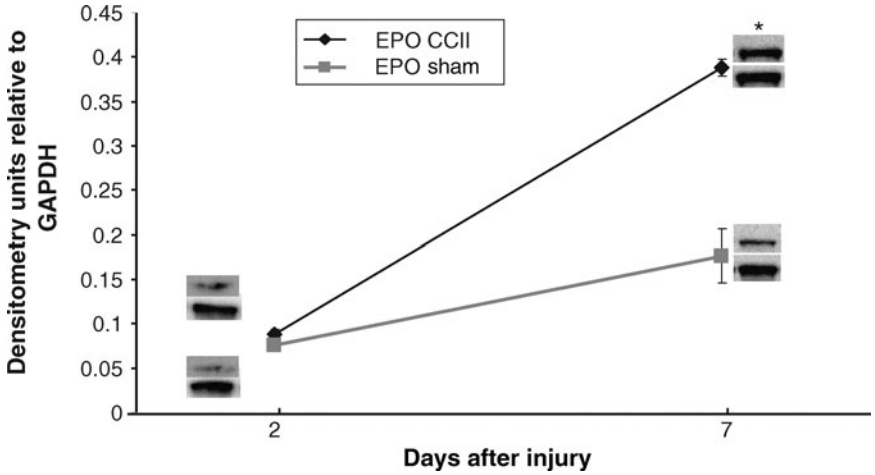

FIG. 8. Graph depicting EPO protein levels in CCI hippocampus ipsilateral to injury (CCII), expressed as densitometry units relative to GAPDH, at PID 2 and 7. CCI EPO protein levels increased relative to sham levels at PID 7. Representative immunoblot images are shown for CCI and sham animals. Results are presented as EPO:GAPDH ratio ± standard error of the mean; $n = 6$; *$p < 0.05$ relative to sham; CCI, controlled cortical impact; GAPDH, glyceraldehyde-3-phosphate dehydrogenase; PID, post-injury day).

IGF-1 protein levels were unchanged at PID 2, 7, and 14, despite increased mRNA expression of IGF-1 at these time points. This apparent discrepancy is not entirely unexpected, as other investigators have reported similar discordance, likely due to the fact that IGF-1 is subject to both transcriptional and post-translational regulation (Olchovsky et al., 1991; Papaconstantinou et al., 2005; Picha et al., 2006).

Similarly to the data on EPO and EPOR expression after TBI in adult animals, we found that EPO and EPOR expression increased in a pTBI model. The differences in timing of this increased expression suggest developmental differences in the endogenous EPO response to TBI. EPO was increased at 12 h after aTBI in rats (Liao et al., 2008), and at 72 h after injury in mice (Anderson et al., 2009), while EPO first increased at PID 7 in our study. Indeed, on the opposite end of the spectrum, aging rodents failed to upregulate cerebral EPO 72 h after CCI (Anderson et al., 2009). In this study, although baseline cerebral EPO levels were higher in aged mice than in adult mice, post-CCI EPO levels were lower, and neurological outcomes worse, in the aged mice than in the adult mice. We thus speculate that perhaps the developing brain with its baseline high levels of EPO is not readily able to upregulate EPO expression in response to TBI.

In our study, the time course of EPOR mRNA expression after CCI was similar to that noted in aTBI studies. In aTBI, EPOR increased early (12 h after injury), and lasted for at least 7 days (Liao et al., 2008).

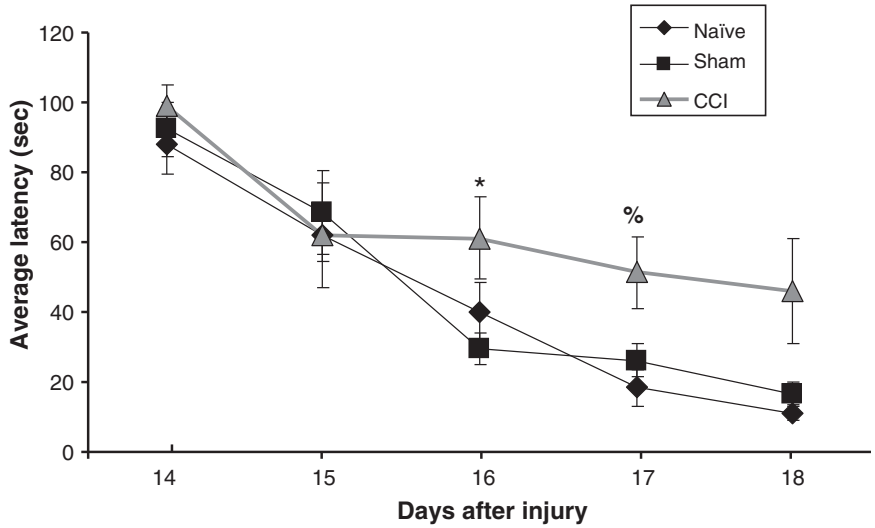

FIG. 9. Graph depicting the average latency to find the hidden platform as a function of day of testing (PID days 14–18) for each group of animals. CCI animals were significantly slower on PID 16 (relative to sham), and on PID 17 (relative to naïve). Latency is expressed in seconds ± standard error of the mean ($n = 6$–8; *$p < 0.05$ relative to sham; %$p < 0.05$ relative to naïve; CCI, controlled cortical impact; PID, post-injury day).

Our study has a number of limitations. First, our findings are limited to immature rodents. No animal model can fully replicate the human condition, yet the results of our study provide useful information for further work in experimental pTBI. Second, we did not test hippocampal subfields separately. Nevertheless, because we used ground whole hippocampi, our data are not skewed to any one region, but rather reflect global hippocampal gene expression. Finally, we did not measure daily mRNA and protein levels, but rather selected time points based on the existing literature. While not exhaustive, our study covers a relatively large number of time points early post-injury relative to similar studies of gene expression in pTBI (Cook et al., 1998), and TBI (Matzilevich et al., 2002; Shah et al., 2006).

In summary, we found that EPO, EPOR, and IGF-1 increased in the hippocampus ipsilateral to CCI in 17-day-old rats, and that these increases occurred at different time points after injury. In support of increased apoptosis in the first 2 days after injury, the bax:bcl2 ratio was increased at PID 1 and 2. Hippocampal IGF-1 increased in these first 2 days after injury while EPO did not increase until PID 7. In contrast, EPOR increased dramatically (to six times sham values) as early as PID 1.

Our findings suggest that administering EPO in the first 2 days after injury, when endogenous EPO is low and EPOR is high, may be a viable therapeutic strategy to protect against early apoptotic cell loss in pTBI. Given the temporal pattern of expression of the genes we studied, we speculate that giving IGF-1 soon after pTBI would have less impact than would giving EPO at that juncture. The known synergy between IGF-1 and EPO in terms of neuronal survival (Digicaylioglu et al., 2004) suggests that giving EPO early would have an even greater benefit than either agent alone. In addition, the robust EPOR response in the first day after injury further supports the potential efficacy of early EPO administration after experimental pTBI. The question of whether or not exogenous EPO will improve hippocampal neuronal survival and function in a model of pTBI clearly warrants future study.

Acknowledgments

Funding for this study was provided by the Primary Children's Medical Center Foundation and the Division of Pediatric Critical Care Medicine, Department of Pediatrics, University of Utah, Salt Lake City, Utah.

Author Disclosure Statement

No competing financial interests exist.

References

Adelson, P.D., Whalen, M.J., Kochanek, P.M., Robichaud, P., and Carlos, T.M. (1998). Blood brain barrier permeability and acute inflammation in two models of traumatic brain injury in the immature rat: a preliminary report. Acta Neurochir. Suppl. 71, 104–106.

Agarwal, M.K., Agarwal, M.L., Athar, M., and Gupta, S. (2004). Tocotrienol-rich fraction of palm oil activates p53, modulates Bax/Bcl2 ratio and induces apoptosis independent of cell cycle association. Cell Cycle (Georgetown, Tex 3), 205–211.

Anderson, J., Sandhir, R., Hamilton, E.S., and Berman, N.E. (2009). Impaired expression of neuroprotective molecules in the HIF-1-alpha pathway following traumatic brain injury in aged mice. J Neurotrauma, 26, 1557–1566.

Anderson, V., Catroppa, C., Morse, S., Haritou, F., and Rosenfeld, J. (2005). Functional plasticity or vulnerability after early brain injury? Pediatrics 116, 1374–1382.

Bayly, P.V., Dikranian, K.T., Black, E.E., Young, C., Qin, Y.Q., Labruyere, J., and Olney, J.W. (2006). Spatiotemporal evolution of apoptotic neurodegeneration following traumatic injury to the developing rat brain. Brain Res. 1107, 70–81.

Bittigau, P., Sifringer, M., Felderhoff-Mueser, U., and Ikonomidou, C. (2004). Apoptotic neurodegeneration in the context of traumatic injury to the developing brain. Exp. Toxicol. Pathol. 56, 83–89.

Bittigau, P., Sifringer, M., Pohl, D., Stadthaus, D., Ishimaru, M., Shimizu, H., Ikeda, M., Lang, D., Speer, A., Olney, J.W., et al. (1999). Apoptotic neurodegeneration following trauma is markedly enhanced in the immature brain. Ann. Neurol. 45, 724–735.

Breese, C.R., D'Costa, A., and Sonntag, W.E. (1994). Effect of in utero ethanol exposure on the postnatal ontogeny of insulin-like growth factor-1, and type-1 and type-2 insulin-like growth factor receptors in the rat brain. Neuroscience 63, 579–589.

Cook, J.L., Marcheselli, V., Alam, J., Deininger, P.L., and Bazan, N.G. (1998). Simultaneous analysis of multiple gene expression patterns as a function of development, injury or senescence. Brain Res. Brain Res. Protoc. 3, 1–6.

Dame, C., Juul, S.E., and Christensen, R.D. (2001). The biology of erythropoietin in the central nervous system and its neurotrophic and neuroprotective potential. Biol. Neonate 79, 228–235.

Digicaylioglu, M., Garden, G., Timberlake, S., Fletcher, L., and Lipton, S.A. (2004). Acute neuroprotective synergy of erythropoietin and insulin-like growth factor I. Proc. Natl. Acad. Sci. USA 101, 9855–9860.

Dixon, C.E., Clifton, G.L., Lighthall, J.W., Yaghmai, A.A., and Hayes, R.L. (1991). A controlled cortical impact model of traumatic brain injury in the rat. J. Neurosci. Methods 39, 253–262.

Dobbing, J., and Sands, J. (1979). Comparative aspects of the brain growth spurt. Early Human Dev. 3, 79–83.

Gao, X., Deng-Bryant, Y., Cho, W., Carrico, K.M., Hall, E.D., and Chen, J. (2008). Selective death of newborn neurons in hippocampal dentate gyrus following moderate experimental traumatic brain injury. J. Neurosci. Res. 86, 2258–2270.

Gobbel, G.T., Bonfield, C., Carson-Walter, E.B., and Adelson, P.D. (2007). Diffuse alterations in synaptic protein expression following focal traumatic brain injury in the immature rat. Childs Nerv. Syst. 23, 1171–1179.

Hickey, R.W., Adelson, P.D., Johnnides, M.J., Davis, D.S., Yu, Z., Rose, M.E., Chang, Y.F., and Graham, S.H. (2007). Cyclooxygenase-2 activity following traumatic brain injury in the developing rat. Pediatr. Res. 62, 271–276.

Hoane, M.R., Kaufman, N., Vitek, M.P., and McKenna, S.E. (2009). COG1410 improves cognitive performance and reduces cortical neuronal loss in the traumatically injured brain. J. Neurotrauma 26, 121–129.

Huh, J.W., Widing, A.G., and Raghupathi, R. (2008). Midline brain injury in the immature rat induces sustained cognitive deficits, bihemispheric axonal injury and neurodegeneration. Exp. Neurol. 213, 84–92.

Langlois, J.A., Rutland-Brown, W., and Thomas, K.E. (2005). The incidence of traumatic brain injury among children in the United States: differences by race. J. Head Trauma Rehabil. 20, 229–238.

Langlois, J.A., Rutland-Brown, W., and Wald, M.M. (2006). The epidemiology and impact of traumatic brain injury: a brief overview. J. Head Trauma Rehabil. 21, 375–378.

Liao, Z.B., Zhi, X.G., Shi, Q.H., and He, Z.H. (2008). Recombinant human erythropoietin administration protects cortical neurons from traumatic brain injury in rats. Eur. J. Neurol. 15, 140–149.

Li, X.S., Williams, M., and Bartlett, W.P. (1998). Induction of IGF-1 mRNA expression following traumatic injury to the postnatal brain. Brain Res. Mol. Brain Res. 57, 92–96.

Lu, D., Mahmood, A., Qu, C., Goussev, A., Schallert, T., and Chopp, M. (2005). Erythropoietin enhances neurogenesis and restores spatial memory in rats after traumatic brain injury. J. Neurotrauma 22, 1011–1017.

Madathil, S.K., Evans, H.N., and Saatman, K.E. (2010). Temporal and regional changes in IGF-1/IGF-1R signaling in the mouse brain after traumatic brain injury. J. Neurotrauma 27, 95–107.

Matzilevich, D.A., Rall, J.M., Moore, A.N., Grill, R.J., and Dash, P.K. (2002). High-density microarray analysis of hippocampal gene expression following experimental brain injury. J. Neurosci. Res. 67, 646–663.

Ochalski, P.G., Fellows-Mayle, W., Hsieh, L.B., Srinivas, R., Okonkwo, D.O., Dixon, C.E., and Adelson, P.D. (2010). Flumazenil administration attenuates cognitive impairment in immature rats after controlled cortical impact. J. Neurotrauma 27, 647–651.

Olchovsky, D., Bruno, J.F., Gelato, M.C., Song, J., and Berelowitz, M. (1991). Pituitary insulin-like growth factor-I content and gene expression in the streptozotocin-diabetic rat: evidence for tissue-specific regulation. Endocrinology 128, 923–928.

Papaconstantinou, J., Deford, J.H., Gerstner, A., Hsieh, C.C., Boylston, W.H., Guigneaux, M.M., Flurkey, K., and Harrison, D.E. (2005). Hepatic gene and protein expression of primary components of the IGF-I axis in long lived Snell dwarf mice. Mechanisms Ageing Dev. 126, 692–704.

Picha, M.E., Silverstein, J.T., and Borski, R.J. (2006). Discordant regulation of hepatic IGF-I mRNA and circulating IGF-I during compensatory growth in a teleost, the hybrid striped bass (*Morone chrysops* x *Morone saxatilis*). Gen. Compar. Endocrinol. 147, 196–205.

Rao, V.L., Dogan, A., Todd, K.G., Bowen, K.K., and Dempsey, R.J. (2001). Neuroprotection by memantine, a non-competitive NMDA receptor antagonist after traumatic brain injury in rats. Brain Res. 911, 96–100.

Rice, D., and Barone, S., Jr. (2000). Critical periods of vulnerability for the developing nervous system: evidence from humans and animal models. Environ. Health Perspect. 108 Suppl. 3, 511–533.

Rink, A., Fung, K.M., Trojanowski, J.Q., Lee, V.M., Neugebauer, E., and McIntosh, T.K. (1995). Evidence of apoptotic cell death after experimental traumatic brain injury in the rat. Am. J. Pathol. 147, 1575–1583.

Robertson, C.L., Saraswati, M., and Fiskum, G. (2007). Mitochondrial dysfunction early after traumatic brain injury in immature rats. J. Neurochem. 101, 1248–1257.

Royo, N.C., LeBold, D., Magge, S.N., Chen, I., Hauspurg, A., Cohen, A.S., and Watson, D.J. (2007). Neurotrophin-mediated neuroprotection of hippocampal neurons following traumatic brain injury is not associated with acute recovery of hippocampal function. Neuroscience 148, 359–370.

Russo, V.C., Gluckman, P.D., Feldman, E.L., and Werther, G.A. (2005). The insulin-like growth factor system and its pleiotropic functions in brain. Endocrine Rev. 26, 916–943.

Saatman, K.E., Contreras, P.C., Smith, D.H., Raghupathi, R., McDermott, K.L., Fernandez, S.C., Sanderson, K.L., Voddi, M., and McIntosh, T.K. (1997). Insulin-like growth factor-1 (IGF-1) improves both neurological motor and cognitive outcome following experimental brain injury. Exp. Neurol. 147, 418–427.

Sanchez, P.E., Navarro, F.P., Fares, R.P., Nadam, J., Georges, B., Moulin, C., Le Cavorsin, M., Bonnet, C., Ryvlin, P., Belmeguenai, A., et al. (2009). Erythropoietin receptor expression is concordant with erythropoietin but not with common beta chain expression in the rat brain throughout the life span. J. Comp. Neurol. 514, 403–414.

Sandberg Nordqvist, A.C., von Holst, H., Holmin, S., Sara, V.R., Bellander, B.M., and Schalling, M. (1996). Increase of insulin-like growth factor (IGF)-1, IGF binding protein-2 and −4 mRNAs following cerebral contusion. Brain Res. Mol. Brain Res. 38, 285–293.

Shah, S.A., Prough, D.S., Garcia, J.M., DeWitt, D.S., and Hellmich, H.L. (2006). Molecular correlates of age-specific responses to traumatic brain injury in mice. Exper. Gerontol. 41, 1201–1205.

Sola, A., Wen, T.C., Hamrick, S.E., and Ferriero, D.M. (2005). Potential for protection and repair following injury to the developing brain: a role for erythropoietin? Pediatr. Res. 57, 110R–117R.

Sonmez, U., Sonmez, A., Erbil, G., Tekmen, I., and Baykara, B. (2007). Neuroprotective effects of resveratrol against traumatic brain injury in immature rats. Neurosci. Lett. 420, 133–137.

Stansberg, C., Vik-Mo, A.O., Holdhus, R., Breilid, H., Srebro, B., Petersen, K., Jorgensen, H.A., Jonassen, I., and Steen, V.M. (2007). Gene expression profiles in rat brain disclose CNS signature genes and regional patterns of functional specialisation. BMC Genomics 8, 94.

Tsuru-Aoyagi, K., Potts, M.B., Trivedi, A., Pfankuch, T., Raber, J., Wendland, M., Claus, C.P., Koh, S.E., Ferriero, D., and Noble-Haeusslein, L.J. (2009). Glutathione peroxidase activity modulates recovery in the injured immature brain. Ann. Neurol. 65, 540–549.

Walter, H.J., Berry, M., Hill, D.J., and Logan, A. (1997). Spatial and temporal changes in the insulin-like growth factor (IGF) axis indicate autocrine/paracrine actions of IGF-I within wounds of the rat brain. Endocrinology 138, 3024–3034.

Yeates, K.O., Armstrong, K., Janusz, J., Taylor, H.G., Wade, S., Stancin, T., and Drotar, D. (2005). Long-term attention problems in children with traumatic brain injury. J. Am. Acad. Child Adolesc. Psychiatry 44, 574–584.

Yeates, K.O., Taylor, H.G., Wade, S.L., Drotar, D., Stancin, T., and Minich, N. (2002). A prospective study of short- and long-term neuropsychological outcomes after traumatic brain injury in children. Neuropsychology 16, 514–523.

Zhang, J., Moats-Staats, B.M., Ye, P., and D'Ercole, A.J. (2007). Expression of insulin-like growth factor system genes during the early postnatal neurogenesis in the mouse hippocampus. J. Neurosci. Res. 85, 1618–1627.

Zhang, X., Chen, Y., Jenkins, L.W., Kochanek, P.M., and Clark, R.S. (2005). Bench-to-bedside review: Apoptosis/programmed cell death triggered by traumatic brain injury. Crit. Care 9, 66–75.

Address correspondence to:
Michelle E. Schober, M.D.
Department of Pediatrics
Division of Critical Care
University of Utah School of Medicine
P.O. Box 581289
Salt Lake City, UT 84158

E-mail: michelle.schober@hsc.utah.edu